Support Information

Binder-Free Hierarchical VS_2 Electrodes for High-Performance Aqueous Zn Ion Batteries towards Commercial Level Mass Loading

Tianpeng Jiao,[a,b,§] Qi Yang,[b,§] Shuilin Wu,[a,c] Zifeng Wang[b], Dong Shen,[a,d] Bin Liu,[a,b] Junye Cheng,[a,b] Hongfei Li,[b] Longtao Ma,[b] Chunyi Zhi,[b,*] and Wenjun Zhang[a,b,*]

[a]*Center of Super-Diamond and Advanced Films (COSDAF), City University of Hong Kong, Tat Chee Avenue, Kowloon, Hong Kong, China. E-mail: apwjzh@cityu.edu.hk*

[b]*Department of Materials Science and Engineering, City University of Hong Kong, Tat Chee Avenue, Kowloon, Hong Kong, China. E-mail: cy.zhi@cityu.edu.hk*

[c]*Department of Mechanical and Biomedical Engineering, City University of Hong Kong, Tat Chee Avenue, Kowloon, Hong Kong, China.*

[d]*Department of Chemistry, City University of Hong Kong, Tat Chee Avenue, Kowloon, Hong Kong, China.*

[§]*These authors contributed equally to this work.*

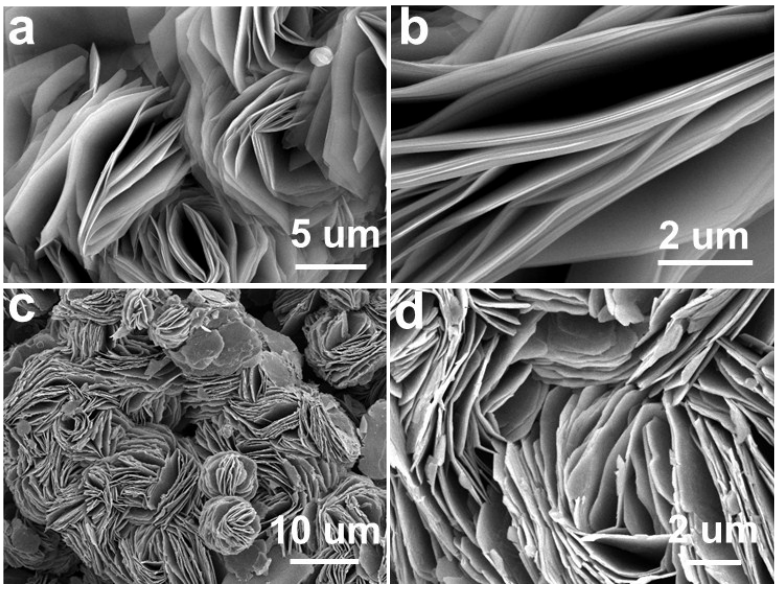

Figure S1. SEM images of (a, b) VS_2@SS electrodes, and (c, d) VS_2 powder.

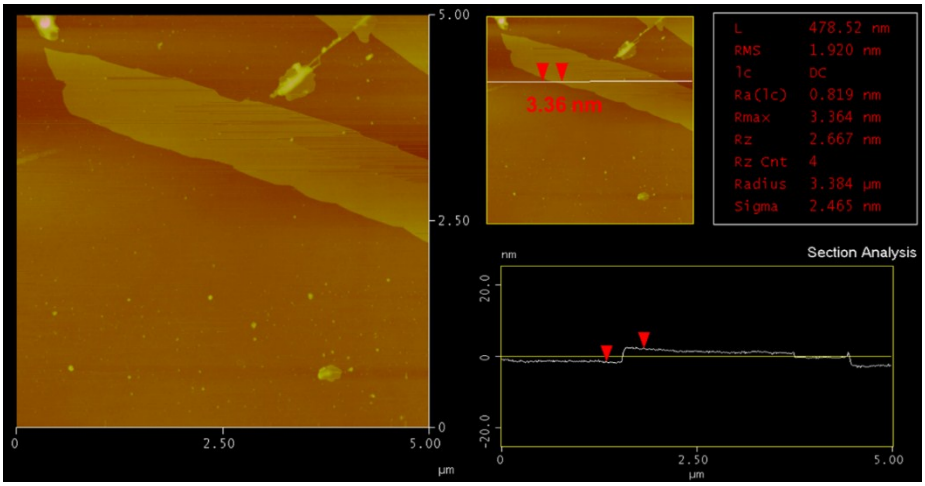

Figure S2. AFM images and the corresponding height profiles of individual VS_2 nanosheets.

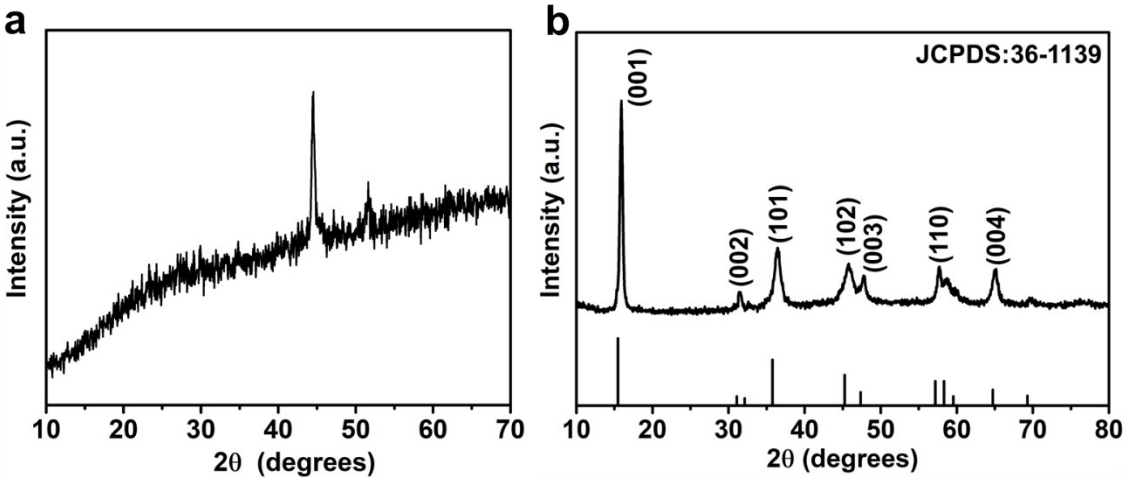

Figure S3. XRD patterns of (a) stainless steel mesh and (b) VS_2 powder.

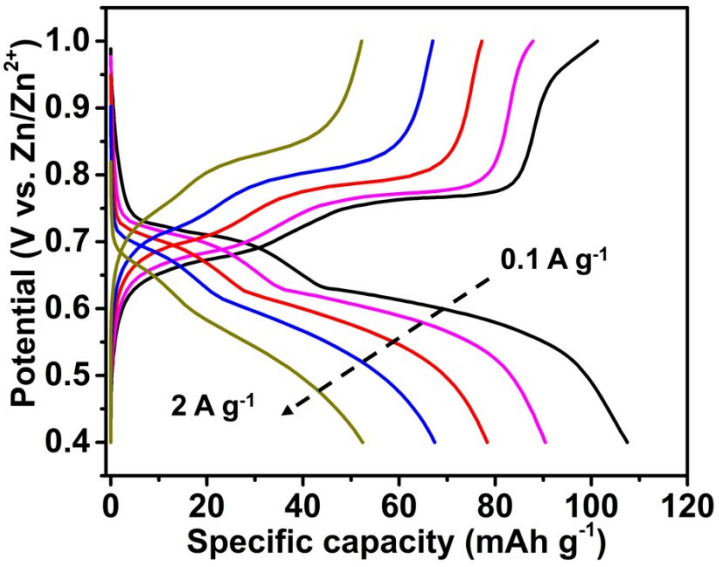

Figure S4. Galvanostatic discharge-charge curves of VS_2 slurry-coated electrode.

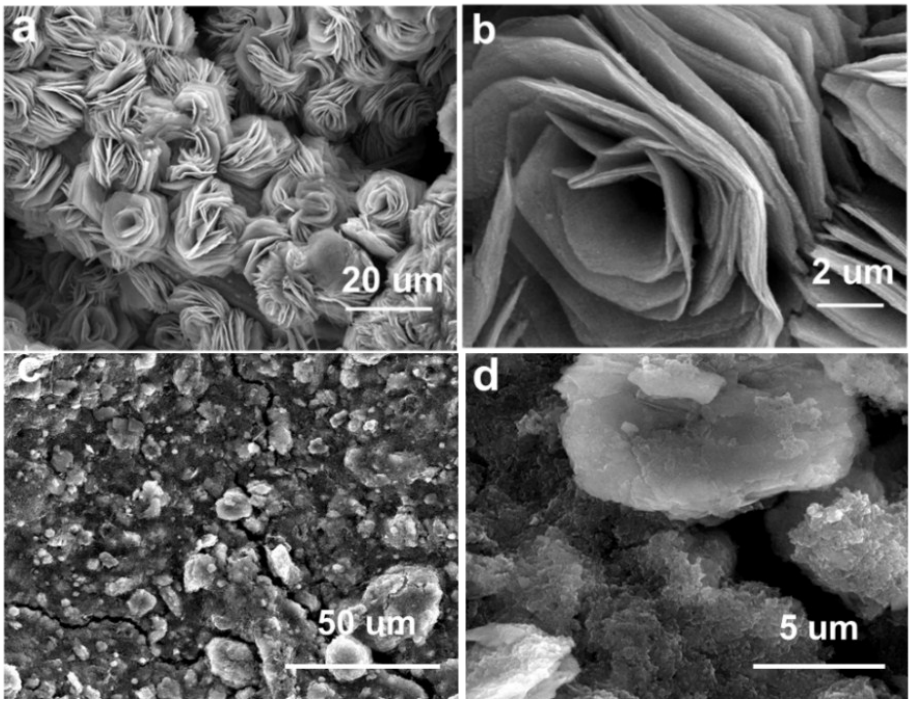

Figure S5. SEM images of (a, b) the VS_2@SS electrode after long-term cycling, and (c, d) the conventional VS_2 slurry-coated electrode after cycling.

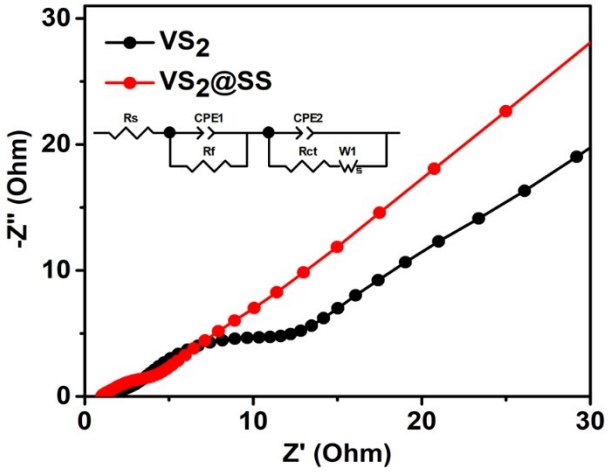

	R_s	R_f	R_{ct}
VS_2@SS electrode	1.1	0.3	1.9
VS_2 slurry-coated electrode	1.8	1	6

Figure S6. Nyquist plots of VS_2@SS and VS_2 slurry-coated electrodes. Inset is the equivalent circuit. The table is the comparison of two electrodes in the calculated values. This circuit is composed of R_s (the solution resistance), R_{ct} (resistance for charge transfer), CPE (constant-phase element) and W (Warburg diffusion process). The parallel circuit R_f CPE1could be related either to the SEI layer or to the bulk resistance. Similar results have been reported in aqueous Li-ion batteries with Li_2SO_4 and $LiNO_3$ electrolyte or superconcentrated LiTFSI electrolyte[1-3].

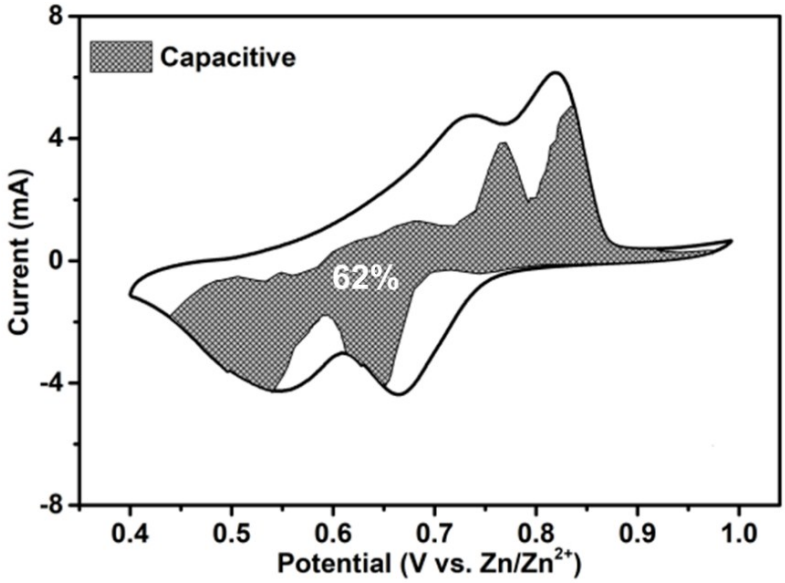

Figure S7. The pseudocapacitive component occupied 62% of total charge storage of VS_2@SS electrode at a scan rate of 0.4 mV s^{-1}.

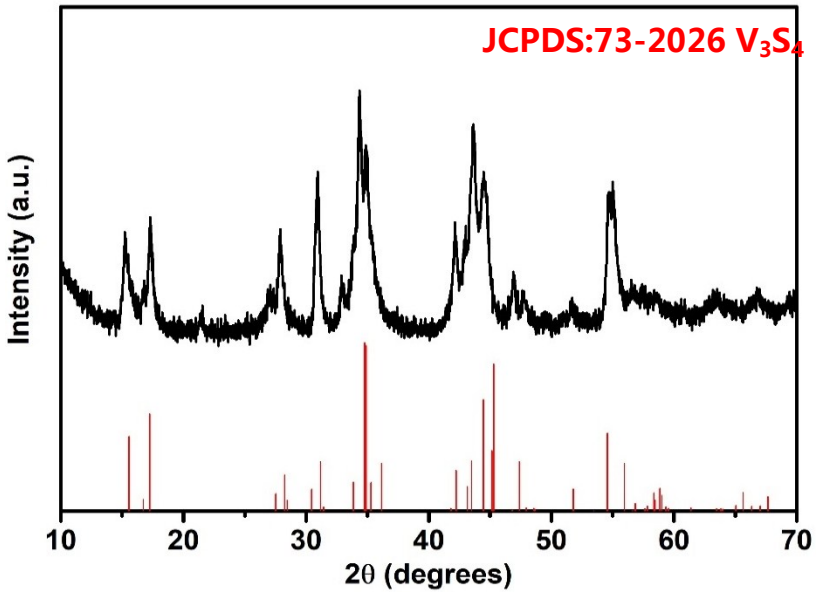

Figure S8. XRD pattern of the fully discharged VS_2@SS electrode.

Figure S9. STEM and the elemental mapping images of the fully discharged VS_2@SS

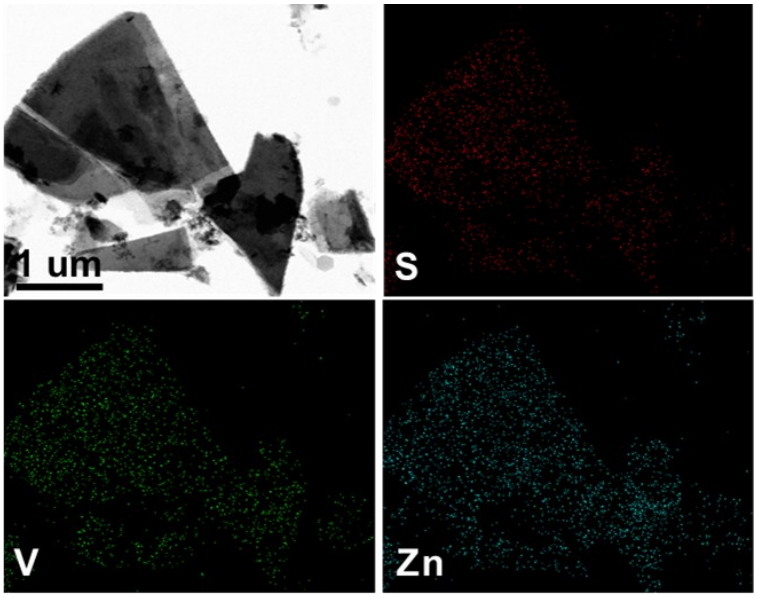

electrode.

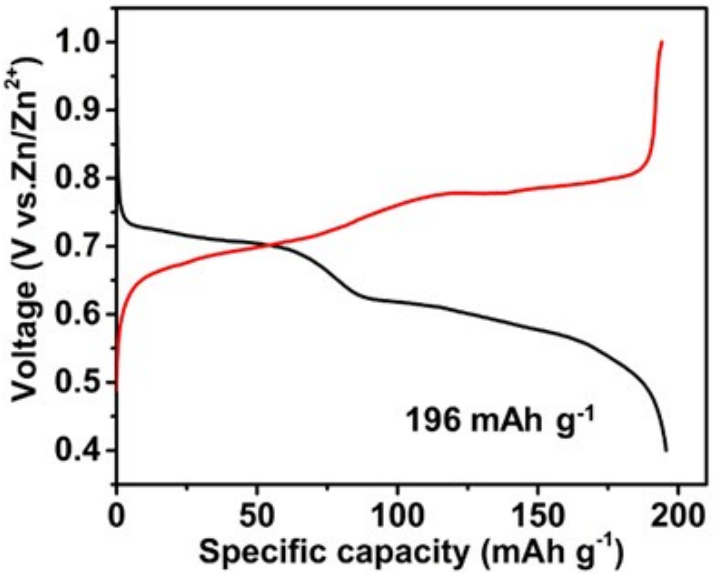

Figure S10. The charge and discharge curves of VS_2@SS electrode at 50 mA g^{-1}.

The intercalation number of Zn^{2+} (x+y) is calculated according to the discharge curve at 50 mA g^{-1} and based on the following equations:

$$x + y = \frac{nC_aM}{C_0}$$

(n is the number of electron exchanged, C_a = 196 mAh g^{-1}, M = 115 g mol^{-1}, C_0 = 26.8 nm M^{-}

[1], F = N_A*e = 96500 C mol^{-1}, 1 Ah = 3600 C)

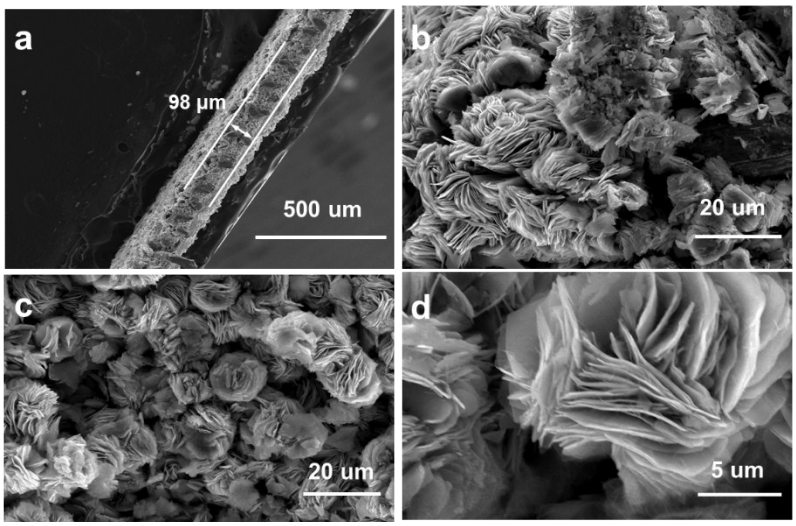

Figure S11. (a) and (b) The cross-section SEM images of VS_2@SS electrode with a mass loading of about 13 mg cm^{-2}. (c) and (d) SEM images of the electrode after cycling.

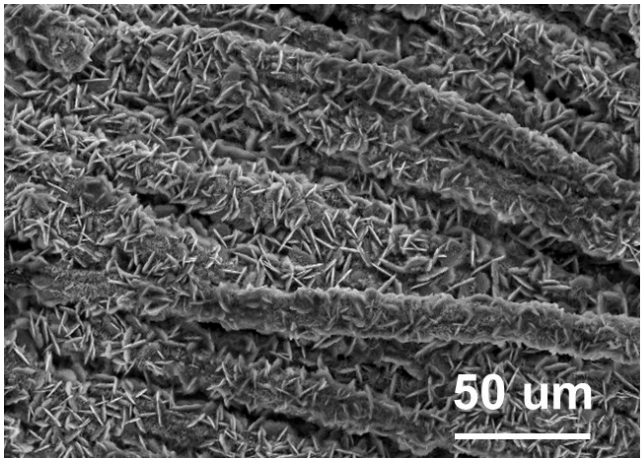

Figure S12. SEM image of the Zn electrodeposited carbon cloth.

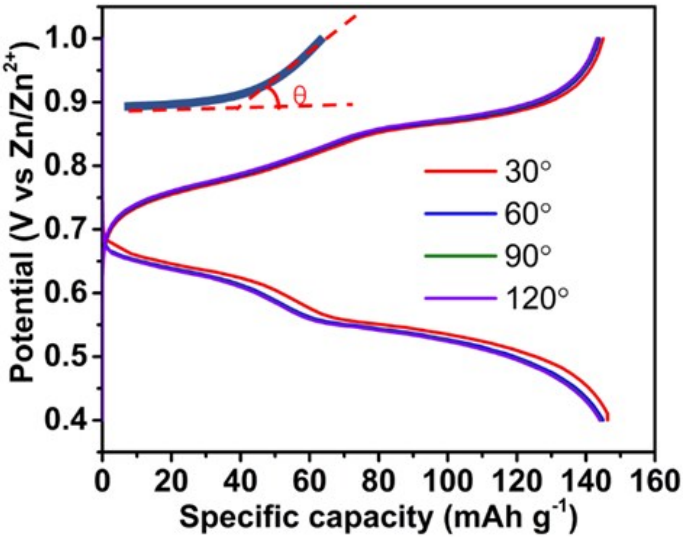

Figure S13. The galvanostatic charge/discharge curves of the flexible solid-state battery under various bending states at 0.5 A g^{-1}. Inset is the definition of the bending angle.

1. R. B. Shivashankaraiah, H. Manjunatha, K. C. Mahesh, G. S. Suresh and T. V. Venkatesha, *Journal of the Electrochemical Society*, 2012, **159**, A1074-A1082.
2. H. Manjunatha, K. C. Mahesh, G. S. Suresh and T. V. Venkatesha, *Electrochimica Acta*, 2011, **56**, 1439-1446.
3. L. M. Suo, D. Oh, Y. X. Lin, Z. Q. Zhuo, O. Borodin, T. Gao, F. Wang, A. Kushima, Z. Q. Wang, H. C. Kim, Y. Qi, W. L. Yang, F. Pan, J. Li, K. Xu and C. S. Wang, *Journal of the American Chemical Society*, 2017, **139**, 18670-18680.